4. G. Jung, J. A. Ledbetter, H. J. Müller-Eberhard, *Proc. Natl. Acad. Sci. U.S.A.* **84**, 4611 (1987); S. A. Möller and R. A. Reisfeld, *Cancer Immunol. Immunother.* **33**, 210 (1991); E. W. Nijhuis, E. van de Wiel-van Kemenade, C. G. Figdor, R. A. van Lier, *ibid.* **32**, 245 (1990).
5. D. Mezzanzanica *et al.*, *Cancer Res.* **51**, 5716 (1991).
6. D. E. Moisier, R. J. Gulizia, S. M. Baird, D. B. Wilson, *Nature* **335**, 256 (1988).
7. H. Takahashi, T. Nakada, I. Puisieux, *Science* **259**, 1460 (1993); A. Hombach *et al.*, *Int. J. Cancer* **55**, 830 (1993).
8. C. Pohl *et al.*, *Int. J. Cancer* **54**, 418 (1993).
9. C. Pohl *et al.*, *ibid.*, p. 820.
10. Peripheral blood lymphocytes were obtained from healthy donors by density centrifugation and were depleted of monocytes and NK cells by adherence to plastic and lysis with leucine methyl ester. For the determination of proliferation, 1×10^6 cells were incubated (48 hours, 37°C) with 1×10^5 L540CY cells, which had been preincubated (1 hour, 4°C) with medium, Bi-mAb CD3-CD30 plus CD28-CD30 (1 μg/ml), CD28-CD30 alone, CD3-CD30 alone, or a mixture of the three parental mAbs CD3 (OKT-3, obtained from ATCC), CD28 (15E8), and CD30 (HRS-3). The percentage of proliferating fluorescein isothyocyanate–conjugated anti-CD3$^+$ cells was determined by flow cytofluorometry after treatment with ribonuclease and DNA staining with propidium iodide as the percentage of CD3$^+$ cells in S, G_2, and M phase.
11. For the induction of cytotoxicity, human PBLs were depleted of NK cells and monocytes (to exclude nonspecific cytotoxicity), adjusted to 1×10^6 cells per well, and prestimulated by incubation in RPMI 1640 plus 20% human serum (72 hours, 37°C) with 1×10^5 CD30$^+$ Hodgkin's-derived L540CY cells or CD30$^-$HPB-ALL cells and Bi-mAb CD3-CD30 (1 μg/ml). After prestimulation, 2.5×10^4 fluorochrome PKH2-labeled vital CD30$^+$ L540CY cells that had been preincubated (1 hour, 4°C) with Bi-mAb or parental mAb (1 μg/ml) were added and cocultured (4 hours, 37°C). The uptake of propidium iodide (2 μg/ml) by avital PKH2$^+$ cells was determined by flow cytofluorometry. The percentage of avital L540CY cells was calculated as the 100-fold ratio of (experimental uptake − spontaneous uptake) to (maximal cell number − spontaneous uptake).
12. Binding of Bi-mAb to tumor cells was demonstrated by immunohistological staining of frozen tissue sections with the APAAP technique (*8*). Human PBL subpopulations in the tumors were identified by staining with biotinylated mAbs and streptavidin-alkaline phosphatase (2 μg/ml).
13. Pathogen-free SCID mice were obtained from the Institut fur Versuchstierzucht, Hannover, Germany. The animal experiments had been approved by the Animal Welfare Committee of the State of North Rhine Westfalia and were performed in accordance with German federal guidelines. Solid L540CY Hodgkin's-derived tumors were established in SCID mice by injection of 1.5×10^7 L540CY cells subcutaneously in the ventral thoracic wall of 4- to 6-week-old female mice. After 10 to 14 days, tumors had grown to a minimal diameter of 0.6 to 0.8 cm. Groups of 10 animals received 50 μg of the Bi-mAbs CD3-CD30 and CD28-CD30 or a mixture of the respective parental antibodies on day 0, followed by intravenous injection of 1×10^7 monocyte- and NK cell–depleted human PBLs after 24 hours (day 1). Tumor diameter was measured with a caliper.
14. H. Dürkop *et al.*, *Cell* **68**, 421 (1992).
15. C. A. Smith *et al.*, *ibid.* **73**, 1349 (1993).
16. W. Jung, unpublished results.
17. S. E. Townsend and J. P. Allison, *Science* **259**, 368 (1993).
18. P. Carde *et al.*, *Eur. J. Cancer* **26**, 474 (1990).
19. P. A. Trail *et al.*, *Science* **261**, 212 (1993).
20. Supported by grants PF 135/3-1 from the Deutsche Forschungsgemeinschaft and Deutsche Krebshilfe. We thank H. Takahashi for providing the protocol for the biodistribution assay of [^{3}H]uridine-labeled human effector cells.

20 August 1993; accepted 18 February 1994

Control of Cell Behavior During Vertebrate Development by *Slug*, a Zinc Finger Gene

M. Angela Nieto, Michael G. Sargent, David G. Wilkinson, Jonathan Cooke*

***Slug*, a vertebrate gene encoding a zinc finger protein of the Snail family, is expressed in the neural crest and in mesodermal cells emigrating from the primitive streak. Early chick embryos were incubated with antisense oligonucleotides to chick *Slug*. These oligonucleotides specifically inhibit the normal change in cell behavior that occurs at the two sites in the emerging body plan in which the gene is expressed. This change, which is the transition from epithelial to mesenchymal character, occurs at the formation of mesoderm during gastrulation and on emigration of the neural crest from the neural tube.**

The events leading to emergence of the body plan in birds closely resemble those of mammalian development but occur in a flat sheet of tissue, the blastoderm, where normal embryo formation can be continuously observed in a simple culture system. We have found that preincubation of blastoderms with antisense oligonucleotides (oligos) can cause specific, transient failure of function of certain early-acting genes. We have screened a complementary DNA (cDNA) library from a 2-day-old chick embryo with a probe from *Xsna* (*1*), the *Xenopus* homolog of the *Drosophila snail* gene (*2*), and isolated clones belonging to genes encoding related zinc finger proteins (*3*). In addition to the chick homolog of *Xsna* and of the mouse gene *Sna* (*4*), we have isolated a gene similar to *Xsna* that we have named *Slug* (Fig. 1). *Slug* displays a dynamic pattern of transcription during early development, which we have analyzed in detail by whole-mount in situ hybridization in embryos of stages 4 to 19 (*5*). This period, from about 18 hours to 3.5 days of development, extends from gastrulation to the onset of differentiation in many organs. Treatment with antisense oligos to the *Slug* gene causes specific developmental failures at the sites of *Slug* transcription. These failures implicate *Slug* in the control of a particular program of cell activity that normally occurs at these sites. The amenability of the early chick embryo to in vitro culture, combined with the use of antisense oligos, may thus provide a powerful tool for analyzing early stages in the genetic control of vertebrate embryogenesis.

The predicted amino acid sequence for the Slug protein (Fig. 1) shows that it contains five zinc fingers in the 3′ half of the protein. The finger region has 89% amino acid identity relative to *Xsna*, and the NH_2-terminal region (residues 1 to 49) has 76% identity. The intervening portion shows only low conservation (30%). In the finger region, Slug is more similar to Escargot (6), another member of the *Drosophila* Snail family, than it is to Snail (80% and 69% conservation, respectively). There are apparently no substantial similarities between *Drosophila* and vertebrates in the nonfinger regions in genes with this distinctive 3′ position and type of zinc finger region.

Slug is transcribed in the flask-shaped epiblast cells that form the flanks of the primitive streak (Fig. 2A). Examination of transversely sectioned material after in situ hybridization suggests that the gene turns on in these cells shortly before they emerge through the disrupted basement membrane at the streak to migrate as mesenchyme in the process of gastrulation. However, *Slug* is never expressed in the strip of tissue that is left in front of the regressing Hensen's node and forms the notochord in the future dorsal midline (Fig. 2B). Unlike other tissue leaving the streak, notochord never enters a freely migrating mesenchymal phase. Even when many anterior somites have formed, *Slug* expression continues in the flanks of the streak-like region that provides a source of tissue for progressive construction of the body posteriorly (Figs. 2F and 3D). *Slug* RNA disappears rather rapidly from cells that have emerged from the front half of the streak, and that are assigned to the somite-forming tissue. Somite formation involves reacquisition of epithelial character. More lateral mesoderm, which retains mesenchymal character, maintains detectable expression of *Slug* for a longer period after its generation at gastrulation, so that this lateral *Slug* signal is visible more anteriorly as the body forms.

M. A. Nieto, Instituto Cajal, Doctor Arce, 37, 28002 Madrid, Spain.
M. G. Sargent, D. G. Wilkinson, J. Cooke, National Institute for Medical Research, Mill Hill, London NW7 1AA, UK.
*To whom correspondence should be addressed.

The other major site of *Slug* transcription, in which greater amounts of RNA are seen, is initially within the nervous system. Transcripts are first detected in the ridges at the edge of the neural plate (Fig. 2C). The most anterior parts, the future forebrain folds, are never positive, but expression spreads back through the remaining neural ridges as somites form and the neural plate continues to roll up into a tube. The onset of transcription at each level roughly keeps pace with the anterior to posterior progression of development, which suggests that the cells expressing *Slug* may be precursors of the neural crest.

Chick neural crest cells originate in the edges of the neural plate and later leave the dorsal neural tube to migrate along defined pathways (*7*). *Slug* transcripts can be detected in the cells of the most dorsal sector of the neural tube (Fig. 2C), and these cells subsequently emigrate from it, following the defined crest pathways (Fig. 2, D through G) and leaving the neural tube *Slug*-negative. At advanced stages (Fig. 2H), *Slug* expression continues at a reduced level in the branchial arches, in the future periocular skeleton and in certain other eye components, and, more posteriorly, in the primordia of the dorsal root ganglia and in the cells migrating through the anterior parts of the sclerotomes. Thus, *Slug* is expressed before and during crest migration and, in many cases, in crest cells that have reached their destination.

One problem in the study of migrating crest cells has been that of distinguishing them from neighboring cells, even though chick-quail chimeras have provided vital information (*8*). Marker antibodies such as those to the glycoprotein epitope HNK-1 and the neurofilament protein NF-M (*9*–*11*) have allowed noninvasive analysis of the neural crest. These may, however, also label certain noncrest structures and be specific to particular crest subpopulations and stages. Thus, comparison of the *Slug* pattern of expression with the pattern produced by immunostaining with an antibody to HNK-1 shows that the antibody labels cells only after they have left the neural tube, as previously described (*11*), whereas *Slug* transcripts are already present in presumptive crest cells before emigration (see matched embryos in Fig. 2I). Unlike NF-M (*11*), *Slug* appears to mark crest throughout the body pattern. It may therefore be the most useful overall marker for neural crest cells that has been found to date.

We designed antisense oligos from two regions of the *Slug* mRNA (positions 3 to 17 for oligo A and 74 to 88 for oligo B, as counted from the translation initiation point) and synthesized them as phosphorothioate derivatives for protection against degradation by nucleases (*12*). For negative controls, we used the corresponding sense sequences and a random mixture of 15-nucleotide oligomer with a nucleotide composition similar to the average composition of the antisense sequences (*13*). Three stages were chosen for antisense treatment: the primitive streak (stage 4), the head process-headfold (stages 6 to 7), and the four- to eight-somite stage (stages 8 to 9). When preincubated with any of the control oligos at a concentration of up to 80 μM before being set up in cultures (*14, 15*), blastoderms at these stages produced normal later embryos that were indistinguishable from those from blastoderms preincubated without oligos or those that developed in ovo (Fig. 3, A, D, G, I, K, M, and O). In contrast, after preincubation with the an-

```
  1  MPRSFLVKKH FNSSKKPNYS ELDTHTVIIS PYLYESYPVP IIPQPEILSS
 51  VAYNPITVWT TTGLLPSPLP NDLSPLSGYP SSLGRVSPPP PSDTSSKDHS
                                  1
101  GSESPISDEE ERIQSKLSDP HAIEAEKFQC GLCNKTYSTF SGLAKHKQLH
              2                               3
151  CDAQSRKSFS CKYCDKEYVS LGALKMHIRT HTLPCVCKIC GKAFSRPWLL
                  4                               5
201  QGHIRTHTGE KPFSCPHCNR AFADRSNLRA HLQTHSDVNK YQCKNCSKTF
251  SRMSLLHKHE ESGCCVAH
```

Fig. 1. Predicted amino acid sequence of Slug cDNA. For cloning and sequencing procedures, see (*3*). The numbers above the sequence mark the positions of the five zinc fingers. Single-letter abbreviations for the amino acid residues are as follows: A, Ala; C, Cys; D, Asp; E, Glu; F, Phe; G, Gly; H, His; I, Ile; K, Lys; L, Leu; M, Met; N, Asn; P, Pro; Q, Gln; R, Arg; S, Ser; T, Thr; V, Val; W, Trp; and Y, Tyr.

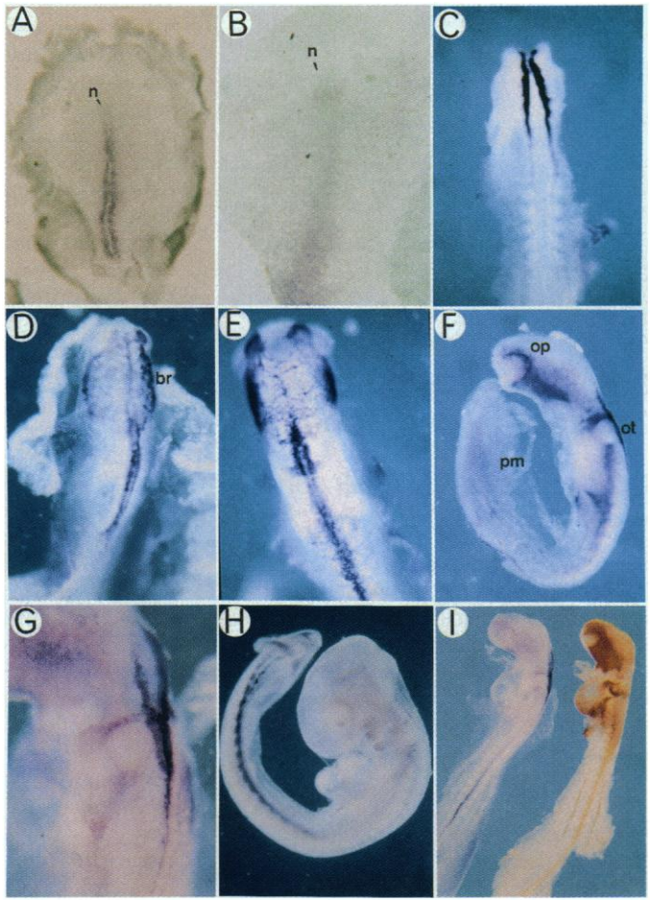

Fig. 2. Pattern of *Slug* expression analyzed by whole mount in situ hybridization. In situ hybridization procedures are given in (*21*). (**A**) In the full-length streak (midgastrulation), *Slug* is expressed at moderate levels as cells transform from epiblastic epithelium into migratory mesoderm. (**B**) At the head process stage (stage 5), it is evident that *Slug* is not expressed in the nonmesenchymal notochordal rod (n) that emerges ahead of Hensen's node. (**C**) By the five-somite stage (stage 8+), more intense expression is seen in the tips of the inward-rolling neural folds at mid- and hindbrain levels. (**D**) In the 10-somite embryo (stage 10), the *Slug*-expressing neural crest has begun emigration at midbrain and branchial levels (br) but, more caudally, is still confined to the neural tube. (**E**) Crest emigration is advanced at periocular and more caudal head levels in the 13-somite embryo and is also under way at cervical and more posterior spinal levels. (**F**) Lateral view of a 16-somite embryo, showing continued crest migration around optic and otic vesicles (op and ot) as well as continued lower level expression in posterior, newly recruited mesoderm (pm). (**G**) *Slug* expression in the hindbrain of a 22-somite embryo shows the characteristic individual crest streams. (**H**) Lateral view of a 35-somite embryo, showing expression in sites populated by crest cells, such as the branchial arches, the periocular region, and the primordia of the dorsal root ganglia. (**I**) Comparison of *Slug* expression and HNK-1 immunostaining in lateral views of 22-somite embryos. The observed patterns of migrating neural crest cells are comparable, but *Slug* expression also reveals cells that remain in the dorsal midline, as in the more posterior spinocaudal region and, partially, in the hindbrain.

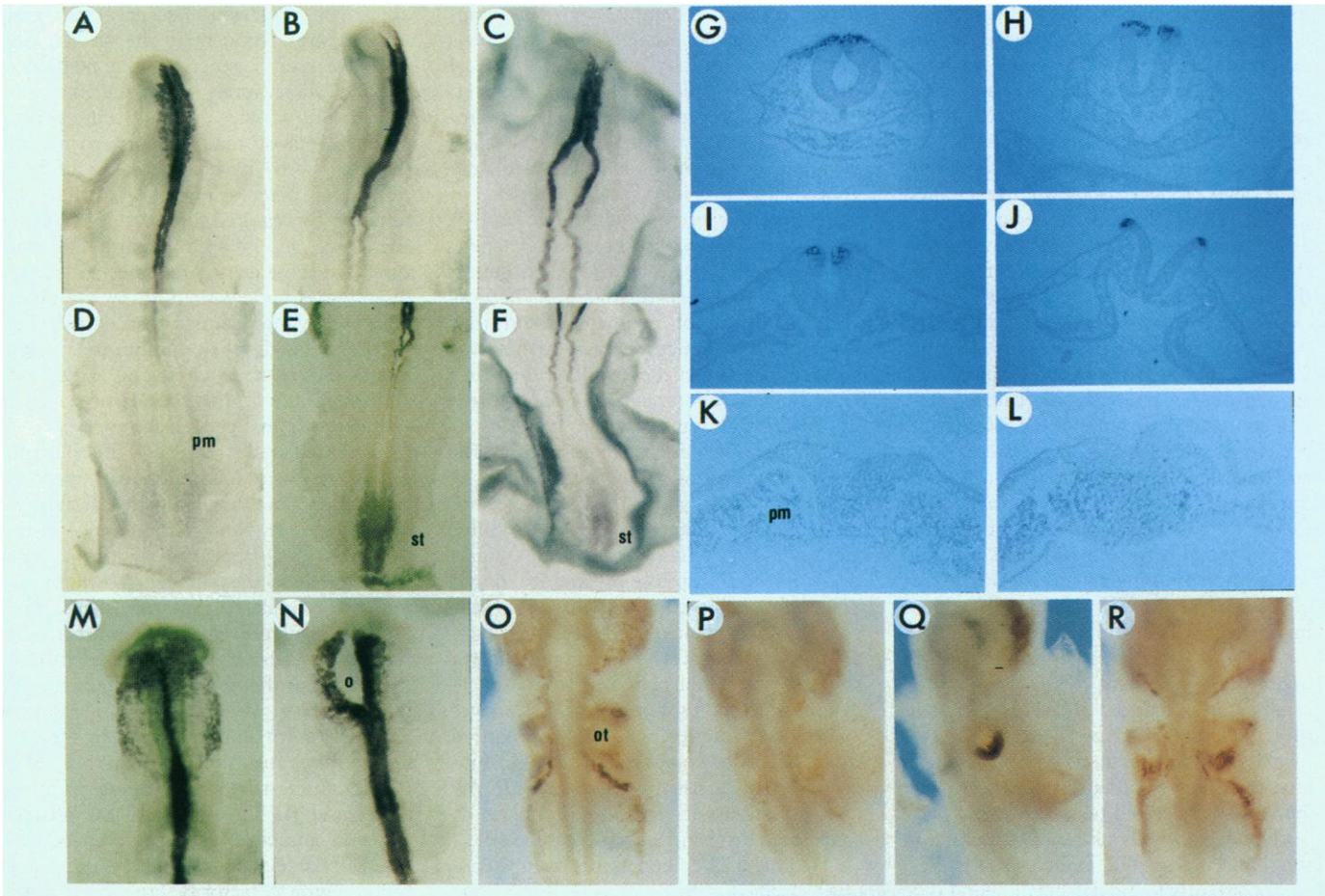

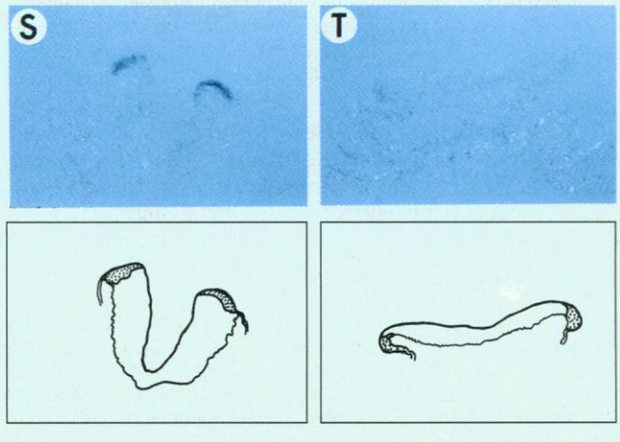

Fig. 3. Anti-*Slug* oligo treatment impairs the epithelial-mesenchymal transition and subsequent cell migration. Details of methods are given in (*15*). Control embryos were all preincubated with the random oligo mixture (*13*). (**A** to **L**) Embryos at the four-somite stage at the end of oligo treatment, analyzed 6 to 8 hours later. (A) Control eight- to nine-somite embryo. (B) Antisense-treated eight- to nine-somite embryo, with lack of normal emigration of crest cells from apposed neural fold regions and a failure to complete neural tube closure. (C) Seven-somite antisense-treated embryo similar to that in (B) but with more severe failure of tube closure. (D to F) More posterior regions of embryos like those in (A) to (C). (F) Abnormally relaxed, open spinocaudal neural tube typical of more severely affected cases. (E and F) Abnormally cell-dense, wrinkled, posterior streak region (st) concentrates the *Slug* signal. In the control embryo (D), signal is distributed as normal in the thin, evenly migrating layer of posterior mesoderm (pm). (G to L) Embedded, transversely sectioned in situ whole mounts of control (eight-somite; G, I, and K) and antisense-treated (seven-somite; H, J, and L) embryos. (G and H) Hindbrain level, showing that release of crest cells from neuroepithelium and closure of the neural tube are paralyzed after antisense treatment. (I and J) Several somites more posterior, neural folds remain widely open after antisense treatment, with epithelial cells less columnarized than normal. Emigration of *Slug*-positive cells has not begun at this level in normal development. (K and L) Root of the normal notochord and neural plate, a region that supplies abundant mesoderm that lightly expresses *Slug* (pm) as development proceeds. There is substantial failure of de-epithelialization and emigration after antisense treatment, which leads to an abnormally jumbled, deep mass of this tissue at the midline, whereas only thin streams escape laterally. (**M**) Control and (**N**) antisense-treated embryos at the 10-somite stage. Antisense treatment prevents the normal extensive crest outflow into branchial and periocular regions, which leaves *Slug*-expressing cells at tube margins. Imperfect suturing left a large opening into the brain (o). (**O** to **R**) Whole mount anti–HNK-1 immunocytochemical preparations at the 15-somite stage, 24 hours after oligo treatment; migrating crest cells are stained brown by HRP-DAB. (O) Control embryo showing normal crest streams from hindbrain rhombomeres around the otic vesicle (ot), as well as the posterior part of the more diffuse anterior crest pattern. (P) Anti-*Slug*–treated embryo with greatly reduced occupancy of these crest pathways. (Q) Anti-*Slug*–treated embryo with more complete paralysis of crest emigration. An HNK-1–positive (non–crest-derived) ear vesicle region is clear. (R) Embryo treated with antisense oligo to chick *snail*, showing normal outflow of crest cells in the hindbrain. (**S** and **T**) Transverse sections through the midbrain neural plate region of embryos after in situ hybridization for *Slug*. Matched stage 8 embryos were fixed 30 min after the end of a 4-hour incubation (*15*) with a random control oligo (*13*) (S) or with anti-*Slug* oligos A and B (13) (T). Structure is poorly preserved in hybridizations done on early embryos immediately after incubation in liquid medium, but accompanying tracings show the nervous system and the *Slug* expression domain. Neural plate shows an abnormally open, relaxed profile in (T), and a pronounced diminution of the *Slug* RNA signal at neural fold tips (Fig. 2C).

tisense oligos, embryos showed morphological abnormalities in the regions of *Slug* expression (Fig. 3). We observed no differences in the kinds and degrees of abnormality obtained with oligos A (40 μM) and B (40 μM) or with a mixture of A and B at a concentration of 12 μM each. Used alone, each oligo produced somewhat less abnormality at 25 μM and none at 12 μM. Taken together, these observations support the specificity of the antisense effects and the synergy to be expected from the use of two sequences from within one gene.

Directly after incubation with oligos for 4 hours, in situ hybridization showed that antisense oligos specifically caused great reduction in the amount of *Slug* RNA present (Fig. 3, S and T). However, *Slug* amounts were later restored to a substantial fraction of normal, which allowed us to follow the altered behavior of cells that express the gene but in which its function was disrupted during an intervening period of development. We examined embryos incubated with control and antisense oligos at stages of somite segmentation 6 to 24 hours after treatment (Fig. 3), and the results are summarized in Table 1. In addition, we immunostained certain embryos for HNK-1 at the more advanced stages after treatment in order to assess the overall amount of emigrated neural crest.

The overall body pattern was normal in the antisense-treated embryos. However, we consistently found defects in neural tube closure between the midbrain and cervical regions (Fig. 3, B, C, H, and N) and impairment or lack of the epithelial-mesenchymal transition in the neural crest (Fig. 3, B and N) and in the emergence of mesoderm from the flanks of the primitive streak (Fig. 3, E, F, and L). In addition, HNK-1 immunocytochemistry revealed the same deficit in the streams of migrating crest cells (Fig. 3, P and Q). The presumptive crest remained integrated into the neuroepithelium dorsally without any sign of the normal transition to mesenchyme (Fig. 3H). It thus prevented proper tube closure, which is normally executed by the *Slug*-negative neural cells lying immediately ventral. In severely affected embryos, in more posterior areas, a different kind of neural abnormality was observed. The neural tube failed to roll in, which left a wide-open boat-shaped structure. The normal thickening of neuroepithelium that results from the lengthening of its cells was reduced throughout the neural cross section (Fig. 3J). This abnormality does not have a straightforward interpretation in terms of the normal *Slug* neural expression pattern. Cells expressing *Slug* are confined to the edges of the folds, and at this axial level and time of development do not yet exhibit mechanical activities (such as crest emigration) whose disruption or absence might affect tube architecture elsewhere. However, in embryos treated with antisense oligos to *Slug*, the paraxial and flanking mesoderm beneath the neural plate was to a variable extent deficient as a result of the above-mentioned interference with primitive streak function. Forces from this mesoderm may normally assist those generated in the neural plate itself to cause the plate to thicken and roll in to form the tube (*16*).

Treatment of embryos with an antisense oligo specific for the related chick *snail* gene causes a different but equally reproducible abnormality (*17*). We believe this to be an additional indicator of the biological meaningfulness of the abnormalities we describe. In genes required very early in development, complete loss of function such as that resulting from experimental knockout in mice may result in the absence of an embryonic axis and thus may be uninformative about gene function. Because of its early transcription throughout the streak, *Slug* could be such a gene, but our method of making observations after graded partial losses of its activity during specific periods of development may have overcome the difficulty posed by complete loss of function. Our observations suggest that *Slug* function is required in cells that release themselves as a group from epithelial structures and subsequently migrate, a sequence of activities undergone both by the neural crest and by mesoderm at gastrulation (*18*). Persistent low-level transcription of *Slug* in lateral mesoderm is consistent with *Slug*'s continued function in the maintenance of the mesenchymal cell phenotype.

The predicted structure of the Slug protein suggests that it functions as a transcription factor and regulates the activity of other genes. In view of the change of cell form that *Slug* appears to control, genes whose products mediate cell-substratum interactions should be explored as candidates for such regulation, direct or indirect (*19*). But other types of genes involved in early patterning of the neural tube could also be targets of *Slug*, which affords an alternative explanation for abnormal form in the neural tube after anti-Slug treatment but before the neural crest is due to emigrate (Fig. 3, C, F, and J). Thus the relation between *Slug* and *dorsalin-1* (*20*), which encodes an intercellular peptide signal of the transforming growth factor β superfamily in the most dorsal portion of the neural tube, may be informative. Finally, pathological activation of *Slug* or of functionally related genes could contribute to the onset of the invasive or metastatic phenotype during the progression of cancers of epithelial origin, because the ability to break through an epithelial basement structure is reminiscent of the mechanism by which mesoderm and the neural crest originate.

Table 1. Results of oligo treatment. We have arbitrarily subdivided the observed degrees of disturbance into two categories. The moderate category includes embryos showing imperfectly closed, crinkled neural folds, inhibition of crest migration, and thickened streak. Embryos in the severe category show thinning of posterior mesoderm, crinkled and widely open spinocaudal neural folds, and severely impaired migration of neural crest and mesodermal cells. Dashes indicate not done.

Developmental stage	Degree of abnormality	Numbers of embryos affected by treatment with			
		No oligo control	Sense oligo control	Random oligo control	Antisense oligos (A, B, and A + B)
4 to 5	None	5	5	15	4
	Moderate	0	0	0	8
	Severe	0	0	0	6
6 to 7	None	5	6	19	0
	Moderate	0	0	0	7
	Severe	0	0	0	15
8 to 9	None	—	—	9	0
	Moderate	—	—	0	5
	Severe	—	—	0	11

REFERENCES AND NOTES

1. M. G. Sargent and M. F. Bennet, *Development* **109**, 963 (1990).
2. J. L. Boulay, C. Dennefield, A. Alberga, *Nature* **330**, 395 (1987).
3. A chicken embryo cDNA library (stage 12 to 15) was made in the Lambda ZAP II vector (Stratagene) and screened at low stringency with a probe from the *Xenopus snail* gene, nucleotides 1 to 695 (*1*). The plasmids containing the cloned cDNAs were excised and sequenced by means of a standard double-stranded dideoxy procedure with synthetic primers. The *Slug* sequence was deposited with the European Molecular Biology Laboratory data bank (accession number x77572).
4. M. A. Nieto, M. F. Bennet, M. G. Sargent, D. G. Wilkinson, *Development* **116**, 227 (1992).
5. V. Hamburger and H. L. Hamilton, *J. Morphol.* **88**, 49 (1951).
6. M. Whiteley, P. D. Noguchi, S. M. Sensabough, W. F. Odenwald, J. A. Kassis, *Mech. Dev.* **36**, 117 (1992).
7. N. Le Douarin, *The Neural Crest* (Cambridge Univ. Press, New York, 1982); A. D'Amico-Martell

and D. M. Noden, *Am. J. Anat.* **166**, 445 (1983); G. Serbedzija, M. Bronner-Fraser, S. F. Fraser, *Development* **106**, 806 (1989).
8. N. Le Douarin, *Dev. Biol.* **30**, 217 (1973); C. Le Lievre and N. Le Douarin, *J. Embryol. Exp. Morphol.* **34**, 125 (1975).
9. G. C. Tucker, H. Aoyama, M. Lipinski, T. Tursz, J. P. Thiery, *Cell Differ.* **14**, 223 (1984).
10. M. Vincent and J. P. Thiery, *Dev. Biol.* **103**, 468 (1984).
11. J. Sechrist, G. N. Serbedzija, T. Scherson, S. E. Fraser, M. Bronner-Fraser, *Development* **118**, 691 (1993).
12. G. Zon and W. J. Stec, in *Oligonucleotides and Analogues*, F. Eckstein, Ed. (Oxford Univ. Press, Oxford, 1991), pp. 87–108.
13. The random oligo mixture was synthesized to have an overall nucleotide composition similar to the average base composition of oligos A and B (Fig. 1) and of an antisense oligo to chick *snail*, according to the following program: A/G G A/G C/T T C/T G A/G A/G C/T C/T C A/G A/G A. The control embryos were treated with this oligo mixture at a concentration of 80 μM. Anti-*Slug* oligos A and B were used at 12 μM.
14. D. A. T. New, *J. Embryol. Exp. Morphol.* **3**, 326 (1955).
15. Blastoderms of the required ages (20 to 30 hours of egg incubation) were explanted as for culture by the technique of New (*14*), in which they rest inverted (endoderm side up), attached as they normally are by their periphery to the vitelline membrane, which is stretched over a ring. The membrane separates the embryo from an underlying pool of growth medium composed of egg albumen (90%) and Pannett and Compton chick saline (10%). For oligo treatment, the blastoderms were detached from their membranes and incubated, ectoderm side up, in 1 ml of a protein-free medium in 35-mm plastic dishes, six to eight per dish. This medium was composed of Hanks balanced salt solution (80%) and Liebovitz TCM (20%) with Ca and Mg^{2+}, each at a concentration of 0.2 mM. Oligos were added from stock concentrates frozen as aliquots in diethyl pyrocarbonate–treated water to give the working concentrations [see text and (*13*)] before incubation for 2 hours at 38°C in humidified air. Blastoderms were then replaced in an inverted position on the original membranes and repositioned while the saline was drained from within the culture ring. The blastoderms reattached and continued to spread on the membranes during the following 6 to 24 hours, until stages of 7 to 15 segmented somites were reached.
16. G. C. Schoenwolf and J. L. Smith, *Development* **109**, 243 (1990).
17. Antisense oligos to chick *snail* have specific effects on somite segmentation but leave neural tube architecture normal (J. Cooke and M. A. Nieto, unpublished observations).
18. R. Bellairs, in *Developmental and Evolutionary Aspects of the Neural Crest*, P. Maderson, Ed. (Wiley, New York, 1987), pp. 123–145.
19. Candidates for regulation by *Slug* could be genes for such molecules as cadherins [M. Takeichi, *Science* **251**, 1451 (1991)] or integrins [(R. O. Hynes, *Cell* **69**, 11 (1992)]. Functional interference studies have shown that matrix-integrin interactions are important for gastrulation [(T. Darribere, K. M. Yamada, K. E. Johnson, J. C. Boucaut, *Dev. Biol.* **126**, 182 (1988)] and for neural crest migration [T. Lallier and M. Bronner-Fraser, *Science* **259**, 692 (1993)], that E-cadherin is involved in the maintenance of epithelial phenotype in epiblast cells [C. A. Burdsal, C. H. Damsky, R. A. Pedersen, *Development* **118**, 829 (1993)], and that impairment of N-cadherin function produces distorted neural tubes and ectopic neural crest cells [M. Bronner-Fraser, J. J. Wolf, B. A. Murray, *Dev. Biol.* **153**, 291 (1992)].
20. K. Basler, T. Edlund, T. M. Jessell, T. Yamada, *Cell* **73**, 687 (1993).
21. Hybridizations were done on paraformaldehyde-fixed embryos by use of a modification of the method described by D. G. Wilkinson and M. A. Nieto [*Methods Enzymol.* **225**, 361 (1993)]. In particular, embryos up to stage 10 were treated with proteinase K for 5 min. Digoxigenin-labeled RNA probes corresponded to nucleotides 1 to 358 and 493 to 1922 from the *Slug* sequence.

22. We thank K. Roberts for help in sequencing *Slug* and M. Placzek and A. Furley for criticism of draft manuscripts. An EDBO short-term fellowship to M.A.N. allowed completion of this work.

22 November 1993; accepted 1 March 1994

Microtubule Dynamics Modulated by Guanosine Triphosphate Hydrolysis Activity of β-Tubulin

Ashley Davis,* Carleton R. Sage, Cynthia A. Dougherty, Kevin W. Farrell

Microtubule dynamic instability underlies many cellular functions, including spindle morphogenesis and chromosome movement. The role of guanosine triphosphate (GTP) hydrolysis in dynamic instability was investigated by introduction of four mutations into yeast β-tubulin at amino acids 103 to 109, a site thought to participate in GTP hydrolysis. Three of the mutations increased both the assembly-dependent rate of GTP hydrolysis and the average length of steady-state microtubules over time, a measure of dynamic instability. The fourth mutation did not substantially affect the rate of GTP hydrolysis or the steady-state microtubule lengths. These results demonstrate that the rate of GTP hydrolysis can modulate microtubule length and hence dynamic instability.

Microtubules are composed of tubulin, an α-β heterodimer that binds GTP exchangeably at the β subunit E site. During microtubule assembly the E-site GTP is hydrolyzed to yield a phosphate ion, which is temporarily bound to the microtubule, and guanosine diphosphate (GDP)–tubulin, which incorporates into the microtubule lattice (*1*). Microtubules are thought to be stabilized by a "cap" (*2*) of GTP-tubulin or [GDP + inorganic phosphate (P_i)]–tubulin subunits at microtubule ends, and the loss of this cap may result in rapid microtubule depolymerization. Random loss and regain of the cap can thus account for the stochastic growing and shortening of microtubules, a process termed dynamic instability, which has been observed both in vitro (*3*) and in vivo (*4*). Dynamic instability is thought to contribute to spindle morphogenesis and the reorganization of microtubule arrays during the cell cycle (*5*).

The tubulin-GTP cap model (*2, 3*) predicts that the GTPase activity of β-tubulin would be important in determining cap size and microtubule dynamics. To investigate the relation between guanosine triphosphatase (GTPase) activity and microtubule dynamics, we combined site-directed mutagenesis with a procedure for purifying assembly-competent tubulin from the yeast *Saccharomyces cerevisiae* (*6, 7*). We report on four mutations directed to the highly conserved region of β-tubulin, Lys^{103}-Gly-His-Tyr-Thr-Glu-Gly^{109} Sequence comparisons (*8*) suggest that this region may be functionally equivalent to the Gly-X-X-X-X-Gly-Lys motif of GTPase superfamily members, which participates in phosphate binding and hydrolysis. We substituted the conserved Lys^{103} with Met, a change that removed the charged amino group but retained the similar overall size and shape of the side group; substitution of Lys with Met in the $p21^{ras}$ Gly-X-X-X-X-Gly-Lys motif reduced that protein's GTPase activity (*9*). We also substituted β-tubulin Thr^{107} with Gly, Lys, or Trp because this amino acid modulates the GTPase activity of other superfamily members (*10*).

Because three of the mutations (Gly^{107}, Lys^{107}, and Trp^{107}) were lethal in haploid cells, we purified tubulin from heterozygous diploid strains (Table 1). In these strains, one β-tubulin gene was full-length (*TUB2* wild type or *TUB2*-derived mutant) and the other (*tub2-590*) was missing the last 12 codons (*11*). The *tub2-590* background allowed immunological detection of full-length β-tubulin with a rabbit polyclonal antibody to the COOH-terminal 12 amino acids of β-tubulin. The tubulin preparations were therefore composed of dimers with full-length (wild type or mutant, as appropriate) and truncated β subunits, in equal amounts (*12*). Purification of tubulin dimers containing only full-length β subunits could be accomplished chromatographically (*13*); however, the yields were too small to make the method routinely useful. The protein derived from each of the heterozygotes assembled into bona fide microtubules, and immunogold staining with the COOH terminal–specific antibody showed that both mutant and wild-type tubulins incorpo-

Department of Biological Sciences, University of California, Santa Barbara, CA 93106, USA.

*To whom correspondence should be addressed.